

DOUBLE MACHINE LEARNING TO ESTIMATE THE EFFECTS OF MULTIPLE TREATMENTS AND THEIR INTERACTIONS

BY QINGYAN XIANG^{1,a}, YUBAI YUAN^{2,c}, DONGYUAN SONG^{3,d}, USMAN J. WUDIL^{4,e},
MUKTAR H. ALIYU^{4,f}, C. WILLIAM WESTER^{4,g}, AND BRYAN E. SHEPHERD^{1,b}

¹*Department of Biostatistics, Vanderbilt University Medical Center* ^aqingyan.xiang@vumc.org, ^bbryan.shepherd@vumc.org

²*Department of Statistics, Penn State University*, ^cyvy5509@psu.edu

³*Department of Genetics and Genome Sciences, University of Connecticut Health Center*, ^ddosong@uchc.edu

⁴*Vanderbilt Institute for Global Health, Vanderbilt University Medical Center* ^eusman.j.wudil@vumc.org,
^fmuktar.aliyu@vumc.org, ^gwilliam.wester@vumc.org

Causal inference literature has extensively focused on binary treatments, with relatively fewer methods developed for multi-valued treatments. In particular, methods for multiple simultaneously assigned treatments remain understudied despite their practical importance. This paper introduces two settings: (1) estimating the effects of multiple treatments of different types (binary, categorical, and continuous) and the effects of treatment interactions, and (2) estimating the average treatment effect across categories of multi-valued regimens. To obtain robust estimates for both settings, we propose a class of methods based on the Double Machine Learning (DML) framework. Our methods are well-suited for complex settings of multiple treatments/regimens, using machine learning to model confounding relationships while overcoming regularization and overfitting biases through Neyman orthogonality and cross-fitting. To our knowledge, this work is the first to apply machine learning for robust estimation of interaction effects in the presence of multiple treatments. We further establish the asymptotic distribution of our estimators and derive variance estimators for statistical inference. Extensive simulations demonstrate the performance of our methods. Finally, we apply the methods to study the effect of three treatments on HIV-associated kidney disease in an adult HIV cohort of 2455 participants in Nigeria.

1. Introduction.

1.1. *Background and motivation.* The development of causal inference methods has made significant progress to address confounding issues in observational studies (Hernan and Robins, 2024; Ding, 2024). However, most causal inference methods focus on a binary treatment, such as comparing the effect of a treatment versus a control (Rosenbaum and Rubin, 1983; Gutman and Rubin, 2015). These methods are inadequate for more complex settings involving multiple treatments, especially when treatment interactions are present. Such settings are not only methodologically challenging but also practically important. For example, in an HIV study, researchers seek to evaluate the side effect of multiple treatments and their interactions on participants' kidney function. To draw meaningful conclusions in this study, it is essential to develop robust causal inference methods that can handle the settings of multiple treatments and their interactions.

Besides the lack of proper methods for multiple treatments, analyzing observational data presents additional challenges. Key issues include high-dimensional confounding covariates (Berisha et al., 2021) and complex confounding relationships—such as non-linear patterns

Keywords and phrases: Causal inference, Machine learning, Multiple treatments, Observational data, Doubly robust estimation.

and higher-order interactions—that influence both treatments and outcomes (Huber, Lechner and Wunsch, 2013; Wan and Mitra, 2018). These challenges complicate the estimation process and increase the potential for bias (D’Amour et al., 2021; Johnstone and Titterington, 2009); the complexity increases further with multiple treatments, as the number of variables and interactions grows. Given these challenges, machine learning methods become a natural choice because of their strengths in modeling high-dimensional data, non-linear patterns, and interactions (Jiang, Gradus and Rosellini, 2020). However, direct use of machine learning in causal inference is not a “free-lunch”. As machine learning methods specialize in prediction instead of estimation, they are subject to overfitting and regularization bias (Neyshabur, Tomioka and Srebro, 2014; Mehrabi et al., 2021; Kernbach and Staartjes, 2022), which can lead to biased estimates of causal effects.

To address aforementioned challenges, we propose a class of new methods for multiple treatments based on double machine learning (DML) (Chernozhukov et al., 2018), a framework that uses machine learning methods to estimate causal effects while overcoming the potential bias induced by regularization and overfitting. Specifically, we contribute to the literature in two broadly applicable settings: (1) a DML partial linear model to estimate the effects of multiple concurrent treatments of different types (binary, categorical, and continuous) and their interactions, and (2) a DML interactive model to estimate the average treatment effect (ATE) across categories of multi-valued regimens. For both setting, we define estimands, propose estimators, and develop corresponding algorithms for effect estimation. Notably, our approach for multiple treatments explicitly models treatment interactions, which are important in practice but have rarely been explored in the causal inference literature. We further describe the asymptotic normality of the proposed estimators and thereby derive the analytical variance estimator for inference.

1.2. The northern Nigeria HIV cohort. We apply our method to investigate the effect of three different treatments on chronic kidney disease in an adult HIV cohort of 2455 participants in northern Nigeria. This application is motivated by the rising incidence of HIV-associated kidney disease, despite the improved survival rates among people with HIV because of the increased use of antiretroviral therapy (ART) (Wudil et al., 2021). Since people with HIV are typically on multiple treatments, studying the side effects of these treatments on kidney function can improve our understanding of HIV-associated kidney disease.

The goal is to estimate the effects of three treatments for HIV and other health conditions, along with their interactions, on kidney function. Kidney function is assessed using the estimated glomerular filtration rate (eGFR), a measure of the severity of chronic kidney disease. The study measured a total of 19 demographic and clinical variables, which may exhibit complex relationships with treatment assignment and kidney function. This application demonstrates how our method addresses challenges arising from multiple treatments, complex confounding structures, and model misspecification.

1.3. Existing work: multiple treatments, or multi-valued treatments. While most causal inference methods focus on binary treatment, recent years have seen a growth in methods for multi-valued treatments in observational studies. Imbens (2000) and Imai and Van Dyk (2004) extended the work of Rosenbaum and Rubin (1983) by proposing the generalized propensity score for multi-valued treatments. Thereafter, many methods for binary treatment have been adapted for multi-valued treatments using the generalized propensity scores: inverse propensity score weighting (IPW) (Feng et al., 2012; McCaffrey et al., 2013), propensity score adjustment (Linden et al., 2016), and propensity score matching (PSM) (Yang et al., 2016; Lopez and Gutman, 2017). In addition to the methods based on propensity scores, other methods have also been extended for multi-valued treatments, including balancing weights

([Li and Li, 2019](#)), Bayes additive regression trees ([Hu et al., 2020, 2022](#)), and targeted maximum likelihood estimation ([Rose and Normand, 2019](#)).

Most of the aforementioned literature does not truly address the settings where multiple treatments are assigned simultaneously. Instead, they focus on “multi-valued treatments,” where each subject receives a single level of treatment that is modeled as a categorical variable $A_i = k$ for $k \in \{1, \dots, K\}$. Therefore, the generalized propensity score is estimated for each category, and the focus is typically on the pairwise contrast, such as ATE between treatment categories. However, in many fields—such as clinical ([Wudil et al., 2021](#)), economic ([Frölich, 2004](#)), and environmental studies ([Zhu et al., 2024](#))—subjects receive multiple treatments at the same time. For example, with two treatments a_1 and a_2 , the causal relationship may take the form:

$$E[Y^{(a_1, a_2)}] = \theta_0 + \theta_1 a_1 + \theta_2 a_2 + \theta_3 a_1 a_2.$$

In this setting, the methods for “multi-valued treatment” show substantial limitations:

- It is not straightforward to estimate θ_3 , the interaction effect between a_1 and a_2 on the outcome.
- It is particularly challenging when a_1 or a_2 is continuous. Research on continuous treatments is still being developed ([Zhu, Coffman and Ghosh, 2015](#); [Kallus and Zhou, 2018](#); [Brown et al., 2021](#)), where a key difficulty is that $P(A = a) = 0$ for a specific a due to its continuity. Moreover, propensity score methods may lead to worse covariate balance for continuous treatments ([Brown et al., 2021](#)).

In this article, we address these limitations by presenting a DML partial linear model (Section 3) that accommodates (1) multiple treatments assigned simultaneously, (2) treatment interactions, and (3) treatments of varying types (binary, categorical, and continuous). To our knowledge, this is the first work to leverage machine learning methods for the robust estimation of causal effects involving both multiple treatments and their interactions.

Related work on such settings remains limited, and most of them overlook the presence of treatment interactions. [Siddique et al. \(2019\)](#) studied effect estimation for multiple concurrent treatments but still treated the combination of treatments as a multi-valued categorical variable. [Wang and Blei \(2019, 2021\)](#) proposed the de-confounder, focusing on causal identification for multiple treatments with unobserved confounders. From a computer science perspective, [Wang et al. \(2024\)](#) reviewed complex treatment settings, including neural network-based methods for multiple treatments ([Qian, Curth and van der Schaar, 2021](#); [Zou et al., 2020](#); [Tanimoto et al., 2021](#)).

Additionally, we describe the DML interactive model for the settings of multi-valued regimens, as detailed in Section 4. While this setting aligns with the classic causal inference literature of multi-valued treatments, we adopt the term “multi-valued regimen” to better reflect its characteristics. See detailed description for this setting in Section 2.

1.4. Structure of this paper. Section 2 describes two settings: (1) mixed-type multiple treatments and (2) multi-valued regimens, along with notation and assumptions. Section 3 presents the DML partial linear model for estimating the effects of multiple treatments and their interactions. Section 4 presents DML interactive model for estimating the pairwise ATE of multiple regimens. Section 5 describes the Neyman orthogonality score function for DML in the context of multiple treatments and multi-valued regimens and derives the analytical variance of our proposed estimator. Section 6 presents simulation studies to demonstrate the performance of DML in different settings. Section 7 applies the DML partial linear model to study the effect of ART level and ART duration on HIV-associated kidney disease. Finally, a discussion section concludes this article.

2. Settings, notation, and assumptions.

2.1. *Settings and notation.* We outline two settings in this article, as illustrated in Figure 1. In the first setting of multiple treatments, subject i receives D treatments simultaneously, denoted as a vector of treatments

$$\mathbf{A}_i = [A_{i1}, A_{i2}, \dots, A_{iD}].$$

Here, A_{id} denotes an individual treatment of different types: binary, categorical, or continuous for $d \in \{1, \dots, D\}$. In addition, we explicitly model the vector of T treatment interactions

$$\mathbf{A}_i^\circ = [A_{i1}^\circ, A_{i2}^\circ, \dots, A_{iT}^\circ],$$

where A_{it}° represents the t -th interaction term, formed as the product of two or more individual treatments, e.g., $A_{i1}^\circ = A_1 A_2$, $A_{i2}^\circ = A_1 A_2 A_3$, etc. The maximum number of interactions is $2^D - D - 1$, but since not all treatments necessarily interact with each other, the actual number of interactions satisfies: $0 \leq T \leq 2^D - D - 1$.

In the second setting of multi-valued regimens, each subject receives one regimen from D regimen categories. Let $R_i = d$ be a categorical indicator of observed treatment status for $d \in \{1, 2, \dots, D\}$; that is, $R_i = d$ if subject i received the d -th regimen. This setting is often referred to as multi-valued treatments in causal inference literature. However, we refer to it as “multi-valued regimen”, since it is common in practice that subjects receive not only a single level of treatment but rather a regimen, which consists of a systemic plan or a combination of treatments.

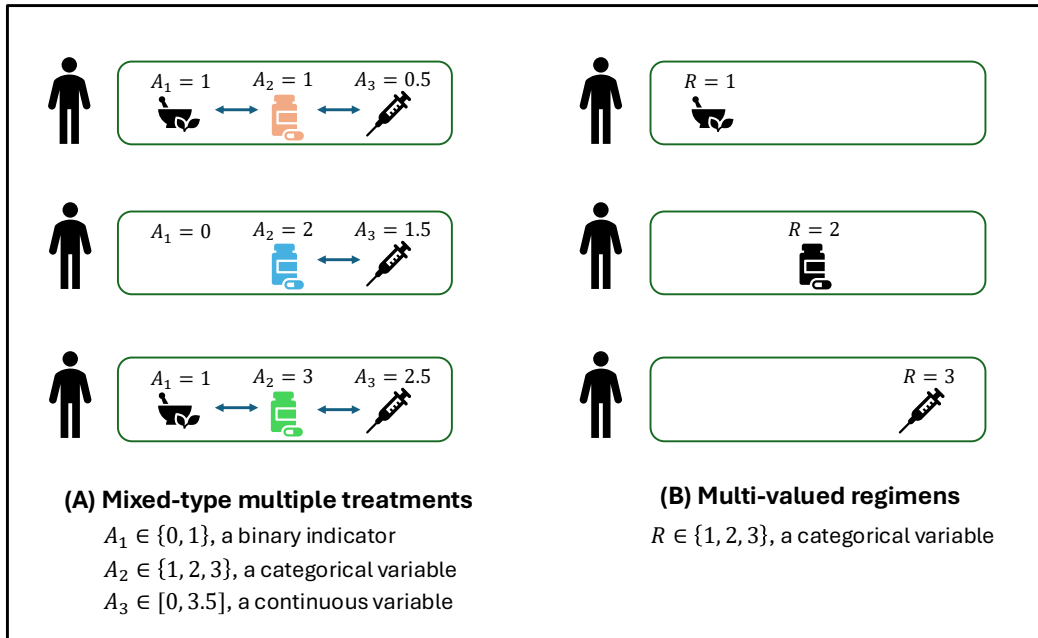


FIG 1. Illustrative settings of (A) multiple treatments and (B) multi-valued regimens. In (A), subjects simultaneously receive multiple treatments of different types, allowing for potential treatment interactions. In (B), subjects receive one category of multi-valued regimens.

Let Y_i denotes the observed continuous outcome for subject i . \mathbf{X}_i denotes a vector of p -dimensional pretreatment confounding covariates. We identify and estimate the causal effects

based on the potential outcome framework (Rosenbaum and Rubin, 1983). For multiple concurrent treatments, each subject i has a set of potential outcomes, denoted as $Y_i^{(a_1, a_2, \dots, a_D)}$, which represents the outcome that would have been observed had subject i received the treatment combination $(A_{i1} = a_1, A_{i2} = a_2, \dots, A_{iD} = a_D)$. Similarly, for multi-valued regimens, subject i has D potential outcomes, where $Y_i^{(r=d)}$ denotes the potential outcome under the d -th regimen for $d \in \{1, \dots, D\}$.

2.2. Assumptions. Under the potential outcome framework, assumptions are required to identify causal effects. For multiple concurrent treatments, we introduce the following assumptions:

- Strong unconfoundedness: $Y_i^{(a_1, a_2, \dots, a_D)} \perp\!\!\!\perp (A_{i1}, A_{i2}, \dots, A_{iD}) | \mathbf{X}_i$, for $(a_1, a_2, \dots, a_D) \in \mathcal{A}$, where \mathcal{A} denotes the space for all possible treatment combinations.
- Positivity: $0 < P((A_{i1}, A_{i2}, \dots, A_{iD}) \in \mathcal{A} | \mathbf{X}_i) < 1$.

Strong unconfoundedness asserts that, given confounders \mathbf{X}_i , potential outcomes under all possible treatment combinations are independent of the assignment of multiple treatments. Positivity asserts that, given \mathbf{X}_i , there is a non-zero probability of observing every possible combination of treatments within \mathcal{A} . Unlike settings with a binary treatment, these assumptions hold jointly across all treatments. It enables identification of causal effects for any combination of treatments and higher-order interactions (e.g., the interaction effect of three treatments simultaneously). Wan and Mitra (2018) also considered similar assumptions.

For multi-valued regimens, since subjects only receive a single category of regimens, the assumptions are different:

- Weak unconfoundedness: $Y_i^{(r=d)} \perp\!\!\!\perp \mathbb{1}_{\{R_i=d\}} | \mathbf{X}_i$, for $d \in \{1, \dots, D\}$.
- Positivity: $0 < P(R_i = d | \mathbf{X}_i) < 1$ for $d \in \{1, \dots, D\}$.

Weak unconfoundedness asserts that, given confounders \mathbf{X}_i , the potential outcome under the d -th regimen is independent of whether subject i received that regimen, as indicated by $\mathbb{1}_{\{R_i=d\}}$. Unlike strong unconfoundedness, weak unconfoundedness only requires the independence to be ‘local’. That is, independence between the potential outcome and the observed regimen holds within each specific regimen category (Imbens, 2000). Similarly, the positivity assumption for multi-valued regimens only requires the marginal probability of observing each category of the regimen is non-zero.

2.3. Identification and estimand. Theorem 1 below shows the identification for settings of multiple treatments:

THEOREM 1. *Under the assumptions of strong unconfoundedness and positivity, the potential outcome under multiple treatments can be identified as follows:*

$$E[Y_i^{(a_{i1}, a_{i2}, \dots, a_{iD})}] = E[E[Y_i | A_{i1} = a_{i1}, A_{i2} = a_{i2}, \dots, A_{iD} = a_{iD}, \mathbf{X}_i]].$$

Appendix Section 1.2 proves Theorem 1, which establishes that the potential outcome under all possible treatments can be identified from observational data. This result enables the identification of the effects of treatment interactions under the partial linear model in Section 3. For example, consider a outcome model with binary treatments a_1 and a_2 :

$$(1) \quad Y_i = \theta_1 A_{i1} + \theta_2 A_{i2} + \theta_3 A_{i1} A_{i2} + g(\mathbf{X}_i) + \varepsilon_i.$$

where $\varepsilon_i \sim N(0, 1)$. Following Theorem 1, the interaction effect θ_3 can be expressed as a combination of average potential outcomes: $\theta_3 = E[Y^{(a_1=1, a_2=1)}] - E[Y^{(a_1=0, a_2=1)}] -$

$E[Y^{(a_1=1, a_2=0)}] + E[Y^{(a_1=0, a_2=0)}]$. Similarly, the estimands for main effects θ_1 and θ_2 can also be expressed as a combination of average potential outcomes. Together, these coefficients allow us to interpret both individual and interaction effects of multiple treatments.

For multi-valued regimens, relevant identification results have been previously studied under the assumptions of weak unconfoundedness and positivity, including Theorem 1 in [Imbens \(2000\)](#) and Lemma 3 in [Yang et al. \(2016\)](#). Though the generalized propensity score is estimated using the full sample of \mathbf{X}_i , the identification can be reached for a specific category of regimen. For example, the potential outcome under b -th regimen is identified as

$$E[Y_i^{(r=b)}] = E[E[Y_i | \mathbb{1}_{\{R_i=b\}}, \mathbf{X}_i]].$$

In this setting, researchers are usually interested in pairwise contrasts between regimens, for example, the ATE between the potential outcomes of the b -th regimen and c -th regimen, with $b, c \in \{1, \dots, D\}$. The estimand for such contrast, denoted as ATE_{bc} , can be expressed as:

$$(2) \quad ATE_{bc} = E[Y_i^{(r=b)} - Y_i^{(r=c)}].$$

We omit the subscript i in the subsequent sections for simplicity.

3. DML partial linear model to estimate effects of multiple treatments and their interactions. Consider the following data generation process. The treatment assignment is given by:

$$(3) \quad \mathbf{A} = \mathbf{m}(\mathbf{X}) + \boldsymbol{\varepsilon}_{\mathbf{A}},$$

where $\mathbf{A} = [A_1, A_2, \dots, A_D]$; each treatment A_d has its own assignment mechanism $m_d(\mathbf{X})$ for $d = 1, \dots, D$, that is:

$$[A_1, A_2, \dots, A_D] = [m_1(\mathbf{X}), m_2(\mathbf{X}), \dots, m_D(\mathbf{X})] + [\varepsilon_{A_1}, \varepsilon_{A_2}, \dots, \varepsilon_{A_D}],$$

with ε_{A_d} as the noise term satisfying $E[\varepsilon_{A_d} | \mathbf{X}] = 0$. Depending on the type of A_d (binary, categorical, or continuous), m_d can be a probabilistic or continuous mapping from \mathbf{X} to A_d . The outcome model is given by:

$$(4) \quad Y = \mathbf{A}^\top \boldsymbol{\theta} + \mathbf{A}^{\circ\top} \boldsymbol{\theta}^\circ + g(\mathbf{X}) + \varepsilon_Y,$$

where \mathbf{A}° is a vector of T interaction terms, as introduced in Section 2,

$$\mathbf{A}^\circ = [A_1^\circ, A_2^\circ, \dots, A_T^\circ];$$

$g(\mathbf{X})$ is a function mapping the confounding covariates \mathbf{X} to \mathbb{R} ; ε_Y is a noise term with $E[\varepsilon_Y | \mathbf{A}, \mathbf{A}^\circ, \mathbf{X}] = 0$. $\boldsymbol{\theta}$ and $\boldsymbol{\theta}^\circ$ are the coefficients for \mathbf{A} and \mathbf{A}° , which have a causal interpretation under strong unconfoundedness, positivity, and Theorem 1.

The treatment interactions \mathbf{A}° cannot be deterministically generated from \mathbf{X} , as the assignment mechanism typically only affects the individual treatments. However, interactions can still be confounded by \mathbf{X} due to its influence on the individual treatment assignments. Since interactions may affect the outcome, they need to be included in the outcome model.

To estimate the population parameters $[\boldsymbol{\theta}^\top, \boldsymbol{\theta}^{\circ\top}]$, we use a “partialing-out” procedure based on the double residual methodology ([Robinson, 1988](#)). This procedure includes two steps: (1) model fitting and (2) residual regression. In the first step, we fit a treatment model for each element of \mathbf{A} and \mathbf{A}° , conditional on \mathbf{X} , to obtain two vector of residuals $\hat{\varepsilon}_{\mathbf{A}}$ and $\hat{\varepsilon}_{\mathbf{A}^\circ}$; we also fit an outcome model of Y , conditional on \mathbf{X} , to obtain the residual $\hat{\varepsilon}_{Y|\mathbf{X}}$. This step can be summarized as:

$$\hat{\varepsilon}_{\mathbf{A}} = \mathbf{A} - \hat{E}[\mathbf{A} | \mathbf{X}], \hat{\varepsilon}_{\mathbf{A}^\circ} = \mathbf{A}^\circ - \hat{E}[\mathbf{A}^\circ | \mathbf{X}],$$

$$\hat{\varepsilon}_{Y|\mathbf{X}} = Y - \hat{E}[Y | \mathbf{X}].$$

$\hat{\varepsilon}_{A^\circ}$ is calculated directly on the entire interaction term instead of computing the residuals from individual treatments separately and then multiplying them. Additionally, $\varepsilon_{Y|X}$ differs from the error term ε_Y in the outcome model (4), where $\varepsilon_{Y|X}$ specifically denotes the residual after conditioning only on \mathbf{X} .

In the second step of the “partialling-out” procedure, we regress the obtained residuals:

$$(5) \quad \hat{\varepsilon}_{Y|X} = \hat{\varepsilon}_A^\top \boldsymbol{\theta} + \hat{\varepsilon}_{A^\circ}^\top \boldsymbol{\theta}^\circ.$$

Consequently, the estimating equations of the residual regression (5) will lead to an estimate of the population parameters $[\boldsymbol{\theta}^\top, \boldsymbol{\theta}^{\circ\top}]$:

$$\begin{bmatrix} \hat{\boldsymbol{\theta}} \\ \hat{\boldsymbol{\theta}}^\circ \end{bmatrix} = \left(E \left[\begin{bmatrix} \hat{\varepsilon}_A \\ \hat{\varepsilon}_{A^\circ} \end{bmatrix} \begin{bmatrix} \hat{\varepsilon}_A^\top & \hat{\varepsilon}_{A^\circ}^\top \end{bmatrix} \right] \right)^{-1} E \left[\begin{bmatrix} \hat{\varepsilon}_A \\ \hat{\varepsilon}_{A^\circ} \end{bmatrix} \hat{\varepsilon}_{Y|X} \right].$$

Because of the complex confounding relationships, we use machine learning methods (e.g. Lasso, tree models, neural network, etc.) to estimate $E[A|\mathbf{X}]$, $E[A^\circ|\mathbf{X}]$, and $E[Y|\mathbf{X}]$. These are commonly referred to as nuisance parameters since they are not our primary parameters of interest. While machine learning methods can introduce regularization bias, the “partialling-out” procedure ensures robust estimation for $[\boldsymbol{\theta}^\top, \boldsymbol{\theta}^{\circ\top}]$ against biases/errors in the nuisance parameter estimation. This key advantage arises from the estimating equations in (5), which satisfy Neyman orthogonality condition (see Section 5 for more details).

Machine learning methods are also subject to overfitting, as their primary goal is prediction rather than estimation. To overcome potential overfitting bias, a core procedure in DML is cross-fitting (Figure 2). The data is split into K folds, and the models for $E[A|\mathbf{X}]$, $E[A^\circ|\mathbf{X}]$, and $E[Y|\mathbf{X}]$ are trained on $K - 1$ folds of the training data. These models are then used to estimate $\hat{E}[A|\mathbf{X}]$, $\hat{E}[A^\circ|\mathbf{X}]$, and $\hat{E}[Y|\mathbf{X}]$ on the held-out data. Therefore, the overfitting bias learned from training data does not affect the held-out data. Then, we calculate the residuals $\hat{\varepsilon}_A$, $\hat{\varepsilon}_{A^\circ}$, and $\hat{\varepsilon}_{Y|X}$ on each held-out fold and aggregate the residuals across all folds. Finally, we plug them into the residual regression (5) to obtain the estimate for $[\boldsymbol{\theta}^\top, \boldsymbol{\theta}^{\circ\top}]$.

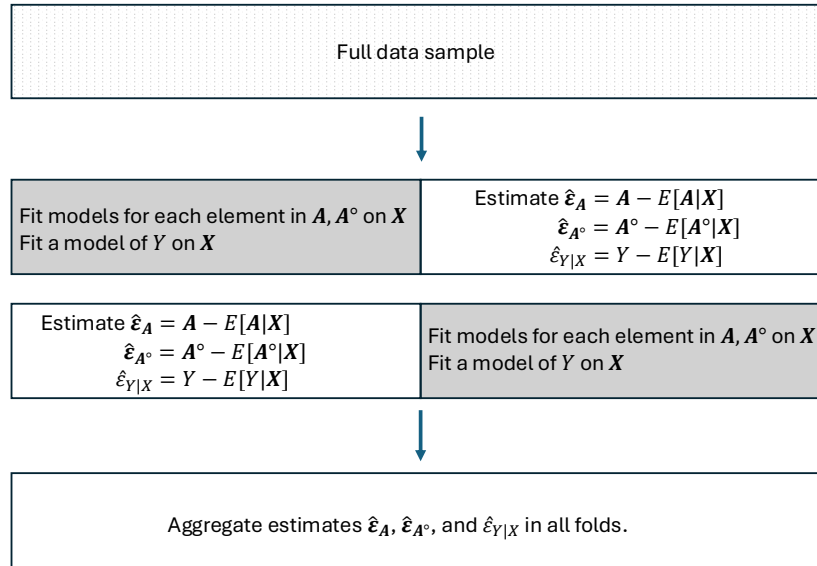


FIG 2. Illustrative figure for a 2-fold cross-fitting in settings of multiple treatments and their interactions.

Algorithm 1 summarizes the procedure of DML partial linear model for estimating the effects of multiple treatments and their interactions. In Step 1.2, one can also fit a multivariate

model for \mathbf{A} and \mathbf{A}° on \mathbf{X} . However, this approach might be difficult when treatments \mathbf{A} differ in types (e.g., binary, categorical, continuous). Therefore, we focus on fitting separate models for each element of \mathbf{A} and \mathbf{A}° .

Algorithm 1 DML partial linear model for multiple treatments and their interactions

Input: Data $\{(\mathbf{X}_i, \mathbf{A}_i, Y_i)\}_{i=1}^N$, where \mathbf{X}_i is a vector of covariates, \mathbf{A}_i is the vector of multiple treatments, and Y_i is the outcome. The subscript i is omitted in the following steps for simplicity.

Step 1: cross-fitting.

1.1 Split the data into K folds.

1.2 Fit models using $K - 1$ folds (training data):

- Fit the model for every element of treatments \mathbf{A} and their interactions \mathbf{A}° to obtain a series of models $E[\mathbf{A}|\mathbf{X}]$ and $E[\mathbf{A}^\circ|\mathbf{X}]$.
- Fit the outcome model $E[Y|\mathbf{X}]$.

1.3 Estimate $\hat{E}[\mathbf{A}|\mathbf{X}]$, $\hat{E}[\mathbf{A}^\circ|\mathbf{X}]$, and $\hat{E}[Y|\mathbf{X}]$ using the held-out fold. Calculate the residuals:

$$\hat{\varepsilon}_{\mathbf{A}} = \mathbf{A} - \hat{E}[\mathbf{A}|\mathbf{X}], \quad \hat{\varepsilon}_{\mathbf{A}^\circ} = \mathbf{A}^\circ - \hat{E}[\mathbf{A}^\circ|\mathbf{X}], \quad \hat{\varepsilon}_{Y|\mathbf{X}} = Y - \hat{E}[Y|\mathbf{X}].$$

1.4 Repeat steps 1.2 - 1.3 for all folds and aggregate the residuals $\hat{\varepsilon}_{\mathbf{A}}, \hat{\varepsilon}_{\mathbf{A}^\circ}, \hat{\varepsilon}_{Y|\mathbf{X}}$ across all folds.

Step 2: estimation. Regress on the residuals from all folds:

$$\hat{\varepsilon}_{Y|\mathbf{X}} = \hat{\varepsilon}_{\mathbf{A}}^\top \boldsymbol{\theta} + \hat{\varepsilon}_{\mathbf{A}^\circ}^\top \boldsymbol{\theta}^\circ.$$

Output: The estimated coefficients are the parameters of interest, $\hat{\boldsymbol{\theta}}$ and $\hat{\boldsymbol{\theta}}^\circ$, reflecting the effect of multiple treatments and their interactions on the outcome.

We now describe the residual calculation (Step 1.3 of Algorithm 1) for both binary treatment and categorical treatment. For a binary treatment $A \in \{0, 1\}$, the residual is computed as

$$\hat{\varepsilon}_A = A - \hat{E}[A|\mathbf{X}] = A - \hat{p}(A|\mathbf{X}).$$

For a categorical treatment $A \in \{0, \dots, L\}$, we estimate the conditional probabilities $\hat{p}(A = l|\mathbf{X})$ for each level $l \in \{0, \dots, L\}$ via a multi-class classification model. We then use dummy variable encoding on A to create binary indicators for each level: $A_{\text{level}:0}$ (reference level), $A_{\text{level}:1}, \dots, A_{\text{level}:L}$. That is, for each level l , we define $A_{\text{level}:l} = 1$ if $A = l$. Residuals for each level are then computed as

$$\tilde{A}_{\text{level}:l} = A_{\text{level}:l} - \hat{E}[A_{\text{level}:l}|\mathbf{X}] = A_{\text{level}:l} - \hat{p}(A = l|\mathbf{X}).$$

Here, $\tilde{\cdot}$ denotes the residual of a variable. Finally, all residuals, except for the reference level $\tilde{A}_{\text{level}:0}$, are included in the residual regression (Step 2 of Algorithm 1). The resulting coefficients can be interpreted as the effects of each treatment level relative to the reference level.

4. DML interactive model to estimate ATE of multi-valued regimens. Consider the following data generation process:

$$(6) \quad P(R = d|\mathbf{X}) = m(\mathbf{X}), \quad d \in \{1, \dots, D\},$$

$$(7) \quad Y = g(R, \mathbf{X}) + \varepsilon_Y,$$

where the equation (6) is the model of the assignment of D regimens and the equation (7) is the outcome model. $m(\mathbf{X})$ is a function mapping the support of \mathbf{X} to the probability of the d -th regimen, for $d = 1, \dots, D$, which is also referred to as generalized propensity score. $g(R, \mathbf{X})$ is a function mapping both R and \mathbf{X} to \mathbb{R} . ε_Y is the error term with

$E[\varepsilon_Y | R, \mathbf{X}] = 0$. This ‘‘interactive model’’ allows the effects of regimens R to be heterogeneous by interacting with \mathbf{X} in the outcome model.

As shown in equation (8) in Section 2.3, the estimand of interest typically is the ATE between the potential outcomes of the b -th regimen and c -th regimen, for $b, c \in \{1, \dots, D\}$. Based on weak unconfoundedness, positivity, and the above data generation process, there are two popular estimators for ATE_{bc} . First, the regression adjusted estimator using the outcome model,

$$\widehat{ATE}_{bc} = E[\hat{g}(r = b, \mathbf{X}) - \hat{g}(r = c, \mathbf{X})],$$

and second, the IPW estimator using the generalized propensity score

$$\widehat{ATE}_{bc} = E \left[\frac{\mathbb{1}_{\{R=b\}}}{\hat{m}_b(\mathbf{X})} Y - \frac{\mathbb{1}_{\{R=c\}}}{\hat{m}_c(\mathbf{X})} Y \right].$$

However, in each of those two estimators, if the outcome model g or the generalized propensity score model m is misspecified, the resulting estimates can be biased and inefficient.

To mitigate the limitations of the previous estimators, a doubly robust approach combines both outcome and propensity score models, which ensures the estimate is consistent if either model is correctly specified. This estimator, referred to as Augmented Inverse Probability Weighting (AIPW) estimator (Robins, Rotnitzky and Zhao, 1995; Bang and Robins, 2005) is given by:

(8)

$$\begin{aligned} \widehat{ATE}_{bc} = & \\ E \left[& \left[\hat{g}(r = b, \mathbf{X}) - \hat{g}(r = c, \mathbf{X}) \right] + \frac{\mathbb{1}_{\{R=b\}} (Y - \hat{g}(r = b, \mathbf{X}))}{\hat{m}_b(\mathbf{X})} - \frac{\mathbb{1}_{\{R=c\}} (Y - \hat{g}(r = c, \mathbf{X}))}{\hat{m}_c(\mathbf{X})} \right]. \end{aligned}$$

The first part, $[\hat{g}(r = b, \mathbf{X}) - \hat{g}(r = c, \mathbf{X})]$, is the difference between the estimated outcomes using the outcome models for b -th and c -th regimens. The latter part resembles the IPW approach; however, instead of weighting the outcomes, it weights the residuals.

Similar to Section 3, we use machine learning methods to estimate m and g , and the estimating equation from (8) satisfies the Neyman orthogonal condition, which overcomes the regularization bias; cross-fitting is used to prevent overfitting bias. For both b -th and c -th regimen, we fit m and g on $K - 1$ folds of the training data and obtain estimates \hat{m} and \hat{g} on the held-out data. Finally, we aggregate estimates \hat{m} and \hat{g} from all folds and use equation (8) to estimate \widehat{ATE}_{bc} . The Algorithm 2 summarizes the whole procedure.

Algorithm 2 DML interactive model for multi-valued regimens

Input: Data $\{(\mathbf{X}_i, R_i, Y_i)\}_{i=1}^N$, where \mathbf{X}_i is a vector of covariates, R_i is the observed regimen, and Y_i is the outcome. The subscript i is omitted in the following steps for simplicity.

Step 1: cross-fitting.

- 1.1 Split the data into K folds.
- 1.2 Fit models using $K - 1$ folds (training data):
 - Fit a multivariate model for generalized propensity score: $P(R = d | \mathbf{X}) = m(\mathbf{X})$, $d \in \{1, \dots, D\}$.
 - Fit the outcome models $Y = g(R = b, \mathbf{X})$ and $Y = g(R = c, \mathbf{X})$ conditioning on $R = b$ and $R = c$, respectively.
- 1.3 Estimate using the \mathbf{X} in the held-out fold:
 - Estimate $\hat{m}_b(\mathbf{X})$ (the propensity of receiving the b -th regimen) and $\hat{m}_c(\mathbf{X})$ (the propensity of receiving the c -th regimen).
 - Estimate $\hat{g}(r = b, \mathbf{X})$ and $\hat{g}(r = c, \mathbf{X})$ for the b -th and c -th regimens, respectively.
- 1.4 Repeat the steps 1.2 - 1.3 for all folds, and aggregate the estimates $\hat{m}_b(\mathbf{X})$, $\hat{m}_c(\mathbf{X})$, $\hat{g}(r = b, \mathbf{X})$, and $\hat{g}(r = c, \mathbf{X})$ across all folds.

Step 2: estimation. Use the doubly robust estimator in equation (8) to estimate the ATE:

$$\widehat{ATE}_{bc} = [\hat{g}(r = b, \mathbf{X}) - \hat{g}(r = c, \mathbf{X})] + \frac{\mathbb{1}_{\{R=b\}}(Y - \hat{g}(r = b, \mathbf{X}))}{\hat{m}_b(\mathbf{X})} - \frac{\mathbb{1}_{\{R=c\}}(Y - \hat{g}(r = c, \mathbf{X}))}{\hat{m}_c(\mathbf{X})}.$$

Output: \widehat{ATE}_{bc} , the average treatment effect between the b -th regimen and c -th regimen.

5. Neyman orthogonality score function and variance estimation. This section discusses the Neyman orthogonal score — key ingredients behind the theory of DML — for multiple treatments and multi-valued regimens. The variance estimation are derived accordingly. We also describe the asymptotic normality for the estimators in both settings and thereby derive the variance estimator for inference.

5.1. Neyman orthogonality score. The Neyman orthogonality ensures the estimation of the effects of multiple treatments/regimens — our primary parameters of interest — remains robust to the bias in the estimation of nuisance parameters (e.g., the treatment model $m(\mathbf{X})$ and the outcome model $g(\mathbf{X})$). To formalize this, we consider the method of moments estimator for our parameter of interest Θ_0 :

$$E[\psi(\mathbf{W}; \Theta_0, \eta_0)] = 0,$$

where ψ is a vector-valued score function that characterizes the moment conditions; \mathbf{W} denotes the sample space: $(\mathbf{X}, Y, \mathbf{A})$ for multiple treatments and (\mathbf{X}, Y, R) for multiple regimens; Θ_0 denotes the true value of parameters of interest, e.g., for multiple treatments and interactions, $\Theta_0^\top = [\theta^\top, \theta^{\circ\top}]$; η_0 denotes the true values of the nuisance parameters;

The *Neyman orthogonality* condition requires the score function ψ satisfies:

$$(9) \quad \partial_t E[\psi(\mathbf{W}; \Theta_0, \eta_0 + t\delta)]|_{t=0} = 0,$$

where $\delta = \eta - \eta_0$ represents deviations of the nuisance parameters from their true values. This condition ensures that bias in estimating η_0 does not affect the moment condition evaluated at Θ_0 , thereby preserving the unbiased estimation for Θ_0 . Furthermore, under conditions in Chernozhukov et al. (2022) the Neyman orthogonality score function in many settings presents double robustness. That is, if at least one component of η is consistently estimated, the estimation for Θ_0 remains unbiased.

The Neyman orthogonality score function for both DML partial linear model and interactive model is linear in Θ , and thereby can be expressed as

$$(10) \quad \psi(\mathbf{W}; \Theta, \eta) = \psi_a(\mathbf{W}; \eta)\Theta + \psi_b(\mathbf{W}; \eta),$$

where $\psi_a(\mathbf{W}; \boldsymbol{\eta})$ is the component linear in θ and $\psi_b(\mathbf{W}; \boldsymbol{\eta})$ is independent of θ . Based on this linear representation, we can also estimate $\boldsymbol{\Theta}$ by solving the moment condition:

$$(11) \quad \boldsymbol{\Theta} = -E[\psi_a(\mathbf{W}; \boldsymbol{\eta})]^{-1}E[\psi_b(\mathbf{W}; \boldsymbol{\eta})]$$

Furthermore, such linearity representation can facilitate the estimation of the variance, which will be presented in the following subsections.

5.2. Neyman orthogonality and variance estimation for multiple treatments and their interactions. In this setting, we propose the DML partial linear model, where the score function is formulated based on the “partialling-out” approach. The Lemma 1 shows that such score function satisfies the Neyman orthogonality condition in (9).

LEMMA 1. *The score function of the DML partial linear model for multiple treatments and interactions,*

$$(12) \quad \psi(\mathbf{W}; \boldsymbol{\Theta}, \boldsymbol{\eta}) = \begin{bmatrix} \mathbf{A} - \mathbf{m}(\mathbf{X}) \\ \mathbf{A}^\circ - \mathbf{m}^\circ(\mathbf{X}) \end{bmatrix} \left(Y - l(\mathbf{X}) - \begin{bmatrix} \mathbf{A} - \mathbf{m}(\mathbf{X}) \\ \mathbf{A}^\circ - \mathbf{m}^\circ(\mathbf{X}) \end{bmatrix}^\top \begin{bmatrix} \boldsymbol{\theta} \\ \boldsymbol{\theta}^\circ \end{bmatrix} \right),$$

satisfies the Neyman orthogonality condition.

In this lemma, $\boldsymbol{\Theta}_0^\top = [\boldsymbol{\theta}^\top, \boldsymbol{\theta}^{\circ\top}]$ and the nuisance parameters $\boldsymbol{\eta} = (\mathbf{m}, \mathbf{m}^\circ, l)$, i.e., $\mathbf{m}(\mathbf{X}) = E[\mathbf{A}|\mathbf{X}]$, $\mathbf{m}^\circ(\mathbf{X}) = E[\mathbf{A}^\circ|\mathbf{X}]$, and $l(\mathbf{X}) = E[Y|\mathbf{X}]$. The Appendix Section 1.2 proves the lemma 1.

Based on this score function, we can also estimate the parameter of interest following equation (10) and (11):

$$\begin{aligned} \begin{bmatrix} \boldsymbol{\theta} \\ \boldsymbol{\theta}^\circ \end{bmatrix} &= -E(\psi_a)^{-1}E(\psi_b) \\ &= E \left[\begin{bmatrix} \mathbf{A} - \mathbf{m}(\mathbf{X}) \\ \mathbf{A}^\circ - \mathbf{m}^\circ(\mathbf{X}) \end{bmatrix} \begin{bmatrix} \mathbf{A} - \mathbf{m}(\mathbf{X}) \\ \mathbf{A}^\circ - \mathbf{m}^\circ(\mathbf{X}) \end{bmatrix}^\top \right]^{-1} E \left[\begin{bmatrix} \mathbf{A} - \mathbf{m}(\mathbf{X}) \\ \mathbf{A}^\circ - \mathbf{m}^\circ(\mathbf{X}) \end{bmatrix} (Y - l(\mathbf{X})) \right] \\ &= E \left[\begin{bmatrix} \boldsymbol{\varepsilon}_A \\ \boldsymbol{\varepsilon}_{A^\circ} \end{bmatrix} [\boldsymbol{\varepsilon}_A^\top \boldsymbol{\varepsilon}_{A^\circ}^\top] \right]^{-1} E \left[\begin{bmatrix} \boldsymbol{\varepsilon}_A \\ \boldsymbol{\varepsilon}_{A^\circ} \end{bmatrix} \boldsymbol{\varepsilon}_{Y|X} \right]. \end{aligned}$$

The third equality in the equation above uses that $\mathbf{A} - \mathbf{m}(\mathbf{X}) = \boldsymbol{\varepsilon}_A$ and $Y - l(\mathbf{X}) = \boldsymbol{\varepsilon}_{Y|X}$. Note that such equation leads to an estimator of the same format as the one derived using the residual regression in Section 3.

Proposition 1 introduces the the asymptotic normality of this estimator for $[\boldsymbol{\theta}^\top, \boldsymbol{\theta}^{\circ\top}]$.

PROPOSITION 1 (Asymptotic normality of DML for multiple treatments and interactions). *Under regularity conditions in the Appendix, the estimator $[\hat{\boldsymbol{\theta}}^\top, \hat{\boldsymbol{\theta}}^{\circ\top}]$ satisfies:*

$$\sqrt{n} \left(\begin{bmatrix} \hat{\boldsymbol{\theta}} \\ \hat{\boldsymbol{\theta}}^\circ \end{bmatrix} - \begin{bmatrix} \boldsymbol{\theta}_0 \\ \boldsymbol{\theta}_0^\circ \end{bmatrix} \right) \xrightarrow{d} N(\mathbf{0}, \boldsymbol{\Sigma}),$$

with asymptotic variance-covariance matrix

$$(13) \quad \boldsymbol{\Sigma} = \mathbf{J}_0^{-1} E \left[\psi(\mathbf{W}; \boldsymbol{\Theta}_0, \boldsymbol{\eta}_0) \psi(\mathbf{W}; \boldsymbol{\Theta}_0, \boldsymbol{\eta}_0)^\top \right] (\mathbf{J}_0^{-1})^\top,$$

where

$$\psi(\mathbf{W}; \boldsymbol{\Theta}_0, \boldsymbol{\eta}_0) = \begin{bmatrix} \boldsymbol{\varepsilon}_A \\ \boldsymbol{\varepsilon}_{A^\circ} \end{bmatrix} \boldsymbol{\varepsilon}_Y,$$

and

$$\mathbf{J}_0 = E[\psi_a(\mathbf{W}, \boldsymbol{\eta}_0)] = -E \left[\begin{bmatrix} \boldsymbol{\varepsilon}_A \\ \boldsymbol{\varepsilon}_{A^\circ} \end{bmatrix} [\boldsymbol{\varepsilon}_A^\top \boldsymbol{\varepsilon}_{A^\circ}^\top] \right].$$

As a consequence of Proposition 1, after computing the estimated score function $\hat{\psi}(\mathbf{W}; \hat{\boldsymbol{\Theta}}, \hat{\boldsymbol{\eta}})$ and $\hat{\mathbf{J}}$, we can estimate the variance using formula (13):

$$\begin{aligned} \hat{\boldsymbol{\Sigma}} &= \hat{\mathbf{J}}^{-1} E \left[\hat{\psi}(\mathbf{W}; \hat{\boldsymbol{\Theta}}, \hat{\boldsymbol{\eta}}) \hat{\psi}(\mathbf{W}; \hat{\boldsymbol{\Theta}}, \hat{\boldsymbol{\eta}})^\top \right] (\hat{\mathbf{J}}^{-1})^\top \\ &= E \left[\begin{bmatrix} \hat{\boldsymbol{\varepsilon}}_A \\ \hat{\boldsymbol{\varepsilon}}_{A^\circ} \end{bmatrix} [\hat{\boldsymbol{\varepsilon}}_A^\top \hat{\boldsymbol{\varepsilon}}_{A^\circ}^\top] \right]^{-1} E \left[\hat{\boldsymbol{\varepsilon}}_Y \begin{bmatrix} \hat{\boldsymbol{\varepsilon}}_A \\ \hat{\boldsymbol{\varepsilon}}_{A^\circ} \end{bmatrix} [\hat{\boldsymbol{\varepsilon}}_A^\top \hat{\boldsymbol{\varepsilon}}_{A^\circ}^\top] \hat{\boldsymbol{\varepsilon}}_Y \right] \left(E \left[\begin{bmatrix} \hat{\boldsymbol{\varepsilon}}_A \\ \hat{\boldsymbol{\varepsilon}}_{A^\circ} \end{bmatrix} [\hat{\boldsymbol{\varepsilon}}_A^\top \hat{\boldsymbol{\varepsilon}}_{A^\circ}^\top] \right]^{-1} \right)^\top. \end{aligned}$$

5.3. Neyman orthogonality and variance estimation for multi-valued regimens. In this setting, we proposed the DML interactive model to estimate the ATE between two regimen categories. The Lemma 2 below shows the score function for this model satisfies the Neyman orthogonality condition.

LEMMA 2. *The score function of the DML interactive model to estimate the ATE,*

$$\begin{aligned} \psi(\mathbf{W}; \theta, \boldsymbol{\eta}) &= [g(r = b, \mathbf{X}) - g(r = c, \mathbf{X})] + \frac{\mathbb{1}_{R=b}(Y - g(r = b, \mathbf{X}))}{m_b(\mathbf{X})} - \frac{\mathbb{1}_{R=c}(Y - g(r = c, \mathbf{X}))}{m_c(\mathbf{X})} - \theta, \end{aligned}$$

satisfies the Neyman orthogonality condition.

In this lemma, the θ denotes parameter of interest – ATE between the b -th regimen and the c -th regimen, $b, c \in 1, \dots, D$. The nuisance parameters $\boldsymbol{\eta} = (m, g)$ are estimated for both b -th and c -th regimens. Appendix Section 1.4 also proves the Lemma 2.

Based on this Neyman orthogonal score, Proposition 2 introduce the the asymptotic normality of the proposed estimator for ATE between two categories of regimen.

PROPOSITION 2 (Asymptotic Normality for DML with multi-valued treatments). *Under regularity conditions in the Appendix, the estimator $\hat{\theta}$ satisfies:*

$$\sqrt{n} (\hat{\theta} - \theta_0) \xrightarrow{d} N(0, \sigma^2),$$

with asymptotic variance

$$(14) \quad \sigma^2 = E [\psi(\mathbf{W}; \theta_0, \boldsymbol{\eta}_0)^2].$$

As a consequence of Proposition 2, after computing the estimated score function $\hat{\psi}(\mathbf{W}; \hat{\theta}, \hat{\boldsymbol{\eta}})$, we can estimate the variance using formula (14):

$$\hat{\sigma}^2 = E [\hat{\psi}(\mathbf{W}; \hat{\theta}, \hat{\boldsymbol{\eta}})^2]$$

6. Simulation studies.

6.1. *Simulation for DML partial linear model.* This subsection evaluates the performance of the DML partial linear model on a simulated dataset. We generate covariates \mathbf{X} of 10 dimensions. Specifically, covariates X_1 to X_5 are drawn independently from $N(0, 1)$, and X_6 to X_{10} are drawn independently from a bernoulli distribution with different probabilities of success. We generate two treatments:

- a binary treatment generated as $A_1 \sim \text{Bernoulli}(\pi_1)$, where $\text{logit}(\pi_1) = m_1(\mathbf{X})$.
- a continuous treatment A_2 generated by $A_2 = m_2(\mathbf{X}) + \varepsilon_{A_2}$, where $\varepsilon_{A_2} \sim N(0, 1)$.

The functions $m_1(\mathbf{X})$ and $m_2(\mathbf{X})$ incorporate a mixture of linear, nonlinear, and interaction effects of the covariates, as detailed in Appendix Section 2.1.

The outcome Y is generated by a model of these two treatments and their interaction, as well as other covariates:

$$Y = \theta_1 A_1 + \theta_2 A_2 + \theta_3 A_1 A_2 + g(\mathbf{X}) + \varepsilon,$$

where ε is a noise term of normal distribution $N(0, 1)$. $g(\mathbf{X})$ is a function of \mathbf{X} that includes various types of effects (linear, non-linear, interaction, etc.), as defined in Appendix Section C. The true effects for treatments are set as

$$\theta_1 = 5, \theta_2 = 15, \text{ and } \theta_3 = 5.$$

We use five different methods to estimate the treatment models and the outcome model: an ordinary regression method, a ℓ_1 -penalized method (Lasso), two tree-based methods (random forest and boosting trees) and a neural network method. To evaluate whether these methods can capture the complex pattern of confounding covariates, the input covariate matrix \mathbf{X} is used in its original form without transformations. The details of parameter choices and model specification are provided in Appendix Section 2.1.

	DML Regression	DML Lasso	DML Random Forest	DML Boosting Trees	DML Neural Network
2-fold cross-fitting					
θ_1	Bias	0.20	0.20	-0.03	-0.03
	rMSE	0.36	0.36	0.18	0.26
θ_2	Bias	0.13	0.10	0.09	-0.12
	rMSE	0.23	0.21	0.15	0.18
θ_3	Bias	-0.27	-0.25	-0.12	-0.13
	rMSE	0.34	0.32	0.18	0.20
5-fold cross-fitting					
θ_1	Bias	0.21	0.20	-0.05	-0.02
	rMSE	0.36	0.36	0.19	0.27
θ_2	Bias	0.13	0.12	0.05	-0.11
	rMSE	0.23	0.22	0.13	0.18
θ_3	Bias	-0.27	-0.26	-0.07	-0.16
	rMSE	0.34	0.33	0.16	0.21

TABLE 1

DML partial linear models for multiple treatments and their interactions, with different machine learning algorithms to fit both treatment and outcome models. θ_1 : the effect of A_1 . θ_2 : the effect of A_2 . θ_3 : the effect of the interaction of A_1 and A_2 .

We use Algorithm 1 to estimate θ_1 , θ_2 and θ_3 , where we consider both 2-fold and 5-fold cross-fitting in our algorithm. Since the estimates can vary depending on the random

sample splits in cross-fitting, we make 50 different splits on this dataset and thereby run 50 estimations. We use the median estimate and median standard error across 50 splits as the final estimates. Table 1 summarizes the biases and rMSE of the simulation results. Based on these results:

- Regarding the bias, tree-based models and the neural network show lower bias than ordinary regression and Lasso, suggesting their strength in capturing nonlinear relationships in the data generation process. The biases for θ_3 are slightly higher than the biases for θ_1 and θ_2 , possibly because the treatment model for interaction term is implicit and more complex than the model of the individual treatment.
- Regarding the rMSE, ordinary regression and Lasso show higher rMSE for θ_1 , θ_2 , and θ_3 compared to other methods. For all methods, the rMSE for θ_1 is relatively higher, suggesting that estimating the binary treatments shows more variability.
- Results between 2-fold and 5-fold cross-fitting are similar.

6.2. Simulations for DML interactive model. Consider the following data generation process of covariates \mathbf{X} of 10 dimensions and regimens R of three categories. Covariates X_1 to X_5 follow a normal distribution of $N(0, 1)$ and X_6 to X_{10} follow a binomial distribution with different probabilities of success. $R = 1, 2$, or 3 , is generated by a multinomial/softmax regression model:

$$R \sim \text{Multinomial}(N, m_1(\mathbf{X}), m_2(\mathbf{X}), m_3(\mathbf{X})),$$

with the probability

$$m_d(\mathbf{X}) = \frac{e^{l_d(\mathbf{X})}}{\sum_{d=1}^3 e^{l_d(\mathbf{X})}},$$

where $l_1(\mathbf{X}) = 1$ and $l_d(\mathbf{X}) = \mathbf{X}^L \beta_d^L + \mathbf{X}^{NL} \beta_d^{NL}$ for $d = 2, 3$. See detailed model specification for $l_d(\mathbf{X})$ in the appendix. In this setting, $R = 1$ can be treated as a control regimen due to $l_1(\mathbf{X}) = 1$ and the relationships between regimens are

$$\begin{aligned} \ln \left(\frac{P(R=2)}{P(R=1)} \right) &= l_2(\mathbf{X}), \\ \ln \left(\frac{P(R=3)}{P(R=1)} \right) &= l_3(\mathbf{X}). \end{aligned}$$

Y is a continuous outcome generated by the outcome model $g(R, \mathbf{X})$ that allows for the interaction between R and \mathbf{X} . Hence the effects of regimens are heterogeneous:

$$Y = g(R, \mathbf{X}) = 5 \cdot \mathbb{1}_{R=2} + 15 \cdot \mathbb{1}_{R=3} \cdot X_9 + \mathbf{X}^L \beta_d^L + \mathbf{X}^{NL} \beta_d^{NL} + \varepsilon,$$

where $\mathbb{1}_{R=3}$ interacts with X_9 . This simulation is to estimate causal estimand ATE_{bc} , as described in Section 4. Here, the true values of these estimands are

$$ATE_{21} = 5, ATE_{31} = 10.5, \text{ and } ATE_{32} = 5.5.$$

We compare the performance of DML interactive model with two other previously proposed methods based on the generalized propensity score: IPW and PSM. In DML, the outcome and treatment models are both fitted using the boosting trees. We use the Python package `DoubleML` to implement DML interactive model (Bach et al., 2022). For IPW and PSM, the generalized propensity score model is estimated using both Generalized Linear Models (GLMs) and the boosting trees, respectively. We use the R package `PSweight` (Zhou et al., 2022) to implement them.

The performance of all methods is measured by relative bias. All methods use the original covariate matrix \mathbf{X} as the input. 200 datasets are generated with $N = 1000$. The Figure 3 shows the simulation results.

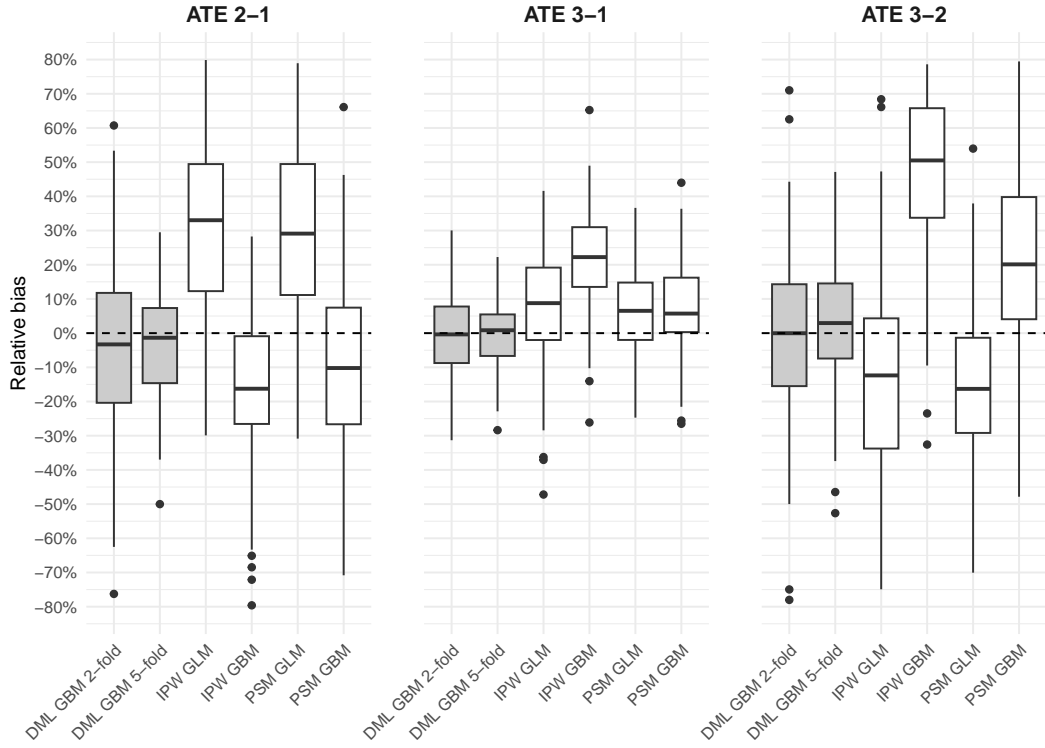


FIG 3. *Relative bias in 200 datasets in three methods for multiple treatment: double machine learning (DML), inverse probability weighting (IPW), and propensity score matching (PSM). In DML, we show results for both 2-fold cross-fitting and 5-fold cross-fitting. In IPW and PSM, the propensity scores are estimated by both generalized linear models (GLM) and gradient boosting machine (GBM). The true treatment effects: $ATE_{2-1} = 5$, $ATE_{3-1} = 10.5$, $ATE_{3-2} = 5.5$.*

The simulation results show that DML interactive model using boosting trees shows the lowest relative bias across all ATE comparisons, and the 5-fold cross-fitting presents a slightly less variability of relative bias than the 2-fold cross-fitting. In contrast, traditional IPW and PSM methods show larger relative biases and greater variability, even when the propensity score is estimated using boosting trees. These findings suggest that DML interactive model account features double robustness by estimating both treatment models and outcome models, which provides more robust estimates for ATE across multiple regimens than traditional methods.

7. Application. We apply the DML partial linear model to estimate the effect of three treatments on HIV-associated kidney disease in an adult HIV cohort in Nigeria. This is a cross-sectional study conducted at Aminu Kano Teaching Hospital in northern Nigeria between 2018 and 2019. The eligibility criteria for the participants includes: (i) HIV-positive, (ii) on ART for a minimum of 6 months, and (iii) between 18 and 70 years of age, as detailed in the study protocol [Aliyu et al. \(2019\)](#). The first visit (baseline) collected demographic and

clinical information from participants. The final visit (5-9 weeks after baseline) collected blood samples to access the estimated glomerular filtration rate (eGFR).

Table 2 summarizes the usage information of three treatments in this study:

1. All participants are on one of three ART regimens of different core agents: Non-Nucleoside Reverse Transcriptase Inhibitor (NNRTI), boosted Protease Inhibitor (bPI), or Dolutegravir (DTG). This is denoted by a three-class categorical variable A_{ART} .
2. Some patients are using Tenofovir Disoproxil Fumarate (TDF) while others are not. This is denoted by a binary variable A_{TDF} .
3. Some patients are using anti-hypertensive (anti-HTN) medications while others are not. This is denoted by a binary variable A_{HTN} .

Because the number of participants on anti-HTN medications are small, it is difficult to estimate interactions between anti-HTN medications and other treatments. We will focus on the interaction between the three-level ART and TDF, i.e., $A_{\text{ART} \times \text{TDF}}^{\circ}$.

		ART (NNRTI) $N = 1435$	ART (bPI) $N = 431$	ART (DTG) $N = 589$
Off TDF	Off anti-HTN	732 (30%)	123 (5.0%)	15 (0.6%)
	On anti-HTN	126 (5.1%)	11 (0.4%)	3 (0.1%)
On TDF	Off anti-HTN	540 (22%)	268 (11%)	498 (20%)
	On anti-HTN	37 (1.5%)	29 (1.2%)	73 (3.0%)

TABLE 2

This table presents number and percentage of the treatment usage under different treatment combinations. The columns are stratified by the three-class ART treatment based on different core agent: Non-Nucleoside Reverse Transcriptase Inhibitor (NNRTI), boosted Protease Inhibitor (bPI), or Dolutegravir (DTG). The rows are stratified by the usage of Tenofovir Disoproxil Fumarate (TDF) and anti-hypertensive (anti-HTN) medications.

We use Y_{eGFR} to denote the outcome eGFR, a measure for chronic kidney disease, with higher eGFR values indicating better kidney function. The vector of covariates \mathbf{X} include: age, sex, ethnicity (Hausa-Fulani, Igbo, Yoruba, or other), risk allele (Apolipoprotein-1), diabetes mellitus status, hypertension status, congestive heart failure status, other comorbid condition status, smoking status, body mass index, systolic and diastolic blood pressure.

7.1. Modeling. We use the DML partial linear model in Algorithm 1 to estimate the effects of A_{ART} , A_{TDF} , A_{HTN} , and the interaction term $A_{\text{ART} \times \text{TDF}}^{\circ}$, on the outcome Y_{eGFR} . An interesting aspect of this application is performing a residual regression that includes A_{ART} —a three-class categorical variable and $A_{\text{ART} \times \text{TDF}}^{\circ}$ —a six-class categorical variable. As mentioned in Section 3, for A_{ART} , we fit a multi-class classification model to estimate the conditional probability of each class of ART treatment. We then use dummy variable encoding on A_{ART} to create a set of binary indicators: $A_{\text{ART:NNRTI}}$ (reference level), $A_{\text{ART:bPI}}$, and $A_{\text{ART:DTG}}$. The residual is computed as

$$\tilde{A}_{\text{ART}:d} = A_{\text{ART}:d} - \hat{E}[A_{\text{ART}:d} | \mathbf{X}] = A_{\text{ART}:d} - \hat{p}[A_{\text{ART}:d} | \mathbf{X}],$$

where $\hat{p}[A_{\text{ART}:d} | \mathbf{X}]$ is the estimated probability of ART type d given covariates \mathbf{X} , for $d \in \{\text{NNRTI, bPI, DTG}\}$. Such approach also applies to the treatment interaction $A_{\text{ART} \times \text{TDF}}^{\circ}$, which is a six-level categorical variable, as detailed in Appendix.

Importantly, we must ensure that the coefficients in the residual regression can be interpreted as effects relative to the reference levels. Since the NNRTI serves as a reference level for the ART treatment, the residual $\tilde{A}_{\text{ART:NNRTI}}$ is omitted from the residual regression model.

The same approach applies to the interaction term: we omit the terms involving either contain the level of NNRTI or the level of “no TDF use”. Therefore, the final residual regression is specified as

$$\begin{aligned}\tilde{Y}_{\text{eGFR}} = & \theta_1 \tilde{A}_{\text{ART: bPI}} + \theta_2 \tilde{A}_{\text{ART: DTG}} + \theta_3 \tilde{A}_{\text{TDF}} + \theta_4 \tilde{A}_{\text{HTN}} \\ & + \theta_5 \tilde{A}_{\text{ART: bPI * TDF}} + \theta_6 \tilde{A}_{\text{ART: DTG * TDF}}.\end{aligned}$$

We use the boosting trees as the learner for both treatment and outcome models to account for complex confounding relationships. We use a 5-fold cross-fitting in the algorithm. To reduce dependence on a single data partition in cross-fitting, we repeat the algorithm 100 times and report the median estimate and the median standard error. 95% confidence interval (CI) are computed based this standard error.

Exposures	Estimated coefficient	SE	95% CI
<i>A_{ART}</i> (reference level: NNRTI)			
bPI	-11.1	1.9	(-14.7, -7.5)
DTG	-20.3	5.1	(-30.0, -10.6)
A _{TDF}	-2.9	1.2	(-5.2, -0.6)
A _{HTN}	-0.6	2.4	(-5.2, 4.0)
<i>A_{ART}*TDF</i> (interaction term)			
Dolutegravir × TDF	6.2	5.2	(-3.7, 16.1)
PI-boosted × TDF	1.3	2.5	(-3.5, 6.0)

TABLE 3

Estimates of coefficients of multiple treatments on kidney function outcome eGFR. A_{ART}: a three-level categorical variable of ART: (1) Non-Nucleoside Reverse Transcriptase Inhibitor (NNRTI), (2) boosted Protease Inhibitor (bPI), or (3) Dolutegravir (DTG). A_{TDF}: a binary indicator of Tenofovir Disoproxil Fumarate (TDF) use. A_{HTN}: a binary indicator of anti-hypertension (HTN) medications use. SE, Standard Error. CI, confidence interval.

		<i>A_{ART} = NNRTI</i> (reference level)	<i>A_{ART} = bPI</i>	<i>A_{ART} = DTG</i>
<i>A_{TDF} = 0</i> (reference level)	<i>A_{HTN} = 0</i>	0	-11.1 (-14.8, -7.4)	-20.3 (-30.3, -10.4)
	<i>A_{HTN} = 1</i>	-0.6 (-5.3, 4.0)	-11.7 (-17.8, -5.6)	-21.0 (-32.0, -9.9)
<i>A_{TDF} = 1</i>	<i>A_{HTN} = 0</i>	-2.9 (-5.3, -0.6)	-7.9 (-18.7, 3.0)	-21.9 (-32.8, -11.1)
	<i>A_{HTN} = 1</i>	-3.6 (-8.9, 1.8)	-8.5 (-20.3, 3.3)	-22.6 (-34.5, -10.6)

TABLE 4

*Estimated effect differences relative to the reference group (*A_{ART} = NNRTI*, *A_{TDF} = 0*, *A_{HTN} = 0*). Each cell reports the contrast between the potential outcome under the treatment combination of the row and column versus that under the reference level. Values are presented as point estimates with 95% confidence intervals in parentheses.*

7.2. Results. Table 3 summaries the estimated coefficients for treatments and their interactions. Table 4 presents the effect differences relative to the reference group ($A_{\text{ART}} = \text{NNRTI}$, $A_{\text{TDF}} = 0$, $A_{\text{HTN}} = 0$). Across all ART strata, switching from NNRTI to either bPI or DTG leads to lower eGFR, particularly for DTG, which consistently shows the largest negative effects. For example, among patients without TDF or anti-HTN, those on DTG-based ART have an estimated eGFR reduction of -20.3 units (95% CI: -30.3, -10.4), while those on bPI-based ART have a reduction of -11.1 (95% CI: -14.8, -7.4).

The effects of TDF and anti-HTN appear additive to ART regimen. For instance, under the NNRTI-based ART, TDF use alone causes a modest but statistically significant reduction (-2.9, 95% CI: -5.3, -0.6), while anti-HTN alone has a nonsignificant effect (-0.6, 95% CI: -5.3, 4.0). Notably, under the DTG-based ART, the combination of TDF and anti-HTN yields the greatest reduction in eGFR (-22.6, 95% CI: -34.5, -10.6). Interestingly, under the bPI-based ART, combining TDF appears to mitigate the negative effect from bPI-based ART. While bPI-based ART alone shows a statistically significant reduction in eGFR (-11.1, 95% CI: -14.8, -7.4), using TDF together results in a smaller and statistically nonsignificant effect (-7.9, 95% CI: -18.7, 3.0).

8. Discussion. Under the strong unconfoundedness assumption, the requirement for joint independence of potential outcomes across all treatments can be relaxed in certain settings. This function serves to help to identify higher order interaction effects (e.g., three-way or higher interactions). However, if the true model only involves pairwise interactions, it suffices to assume pairwise conditional independence of potential outcomes across pairwise combinations of treatments.

The DML partial linear model implicitly assumes additive relationships between the multiple treatments and the outcome. This structure is not overly restrictive as it is close to traditional multi-way ANOVA, where treatments and their interactions are modeled linearly. Like ANOVA, the partial linear model distinguishes between main effects and interaction effects of treatments, allowing interaction effect to be interpreted conditional on the main treatments. However, DML further extends this structure by using machine learning to learn complex confounding models, improving the robustness of the estimates for treatment effects.

The intuition behind the “partialling-out” procedure in DML partial linear model is as follows: think of $E[Y | \mathbf{X}]$ as projecting Y onto the space of \mathbf{X} . The residuals, $\hat{\varepsilon}_{Y|\mathbf{X}}$, are orthogonal (or independent) to the space of \mathbf{X} , effectively “de-biasing” Y from \mathbf{X} . Similarly, the residuals $\hat{\varepsilon}_{\mathbf{A}}$ and $\hat{\varepsilon}_{\mathbf{A}^\circ}$ represent the “de-biased” residuals, removing its dependence on \mathbf{X} . Then, regressing the residuals lead to an estimating equations of $[\theta^\top, \theta^{\circ\top}]$ that is free from confounding induced by \mathbf{X} .

In sum, we describe (1) the DML partial linear model to estimate multiple treatments and their interactions and (2) the DML interactive to estimate the ATE between two category of multi-valued regimens. We show that the score function of these models satisfy the Neyman orthogonality condition and thereby derive the variance estimator. The simulation studies, including semi-synthetic data and fully synthetic data, demonstrate the performance of our proposed methods. The application shows that the proposed DML methods provides a useful tool for robust estimates of multiple treatments leveraging strengths of machine learning methods.

Acknowledgments. Bryan E. Shepherd is funded by R01AI093234 and R37AI093234. The Nigeria HIV study was funded by U01DK112271 and R01DK127912. The findings and conclusions are those of the authors and do not necessarily represent the official position of the National Institutes of Health, the Department of Health and Human Services or the government of the United States of America. The authors would like to thank the participants from Nigeria HIV study for their involvement.

SUPPLEMENTARY MATERIAL

The Appendix includes the additional proofs, simulation details, and application details.

REFERENCES

ALIYU, M. H., WUDIL, U. J., INGLES, D. J., SHEPHERD, B. E., GONG, W., MUSA, B. M., MUHAMMAD, H., SANI, M. U., ABDU, A., NALADO, A. M. et al. (2019). Optimal management of HIV-positive adults at risk for kidney disease in Nigeria (R enal R isk R eduction “R3” Trial): protocol and study design. *Trials* **20** 1–11.

BACH, P., CHERNOZHUKOV, V., KURZ, M. S. and SPINDLER, M. (2022). DoubleML – An Object-Oriented Implementation of Double Machine Learning in Python. *Journal of Machine Learning Research* **23** 1–6.

BANG, H. and ROBINS, J. M. (2005). Doubly robust estimation in missing data and causal inference models. *Biometrics* **61** 962–973.

BERISHA, V., KRANTSEVICH, C., HAHN, P. R., HAHN, S., DASARATHY, G., TURAGA, P. and LISS, J. (2021). Digital medicine and the curse of dimensionality. *NPJ digital medicine* **4** 153.

BROWN, D. W., GREENE, T. J., SWARTZ, M. D., WILKINSON, A. V. and DESANTIS, S. M. (2021). Propensity score stratification methods for continuous treatments. *Statistics in medicine* **40** 1189–1203.

CHERNOZHUKOV, V., CHETVERIKOV, D., DEMIRER, M., DUFLO, E., HANSEN, C., NEWHEY, W. and ROBINS, J. (2018). Double/debiased machine learning for treatment and structural parameters.

CHERNOZHUKOV, V., ESCANCIANO, J. C., ICHIMURA, H., NEWHEY, W. K. and ROBINS, J. M. (2022). Locally robust semiparametric estimation. *Econometrica* **90** 1501–1535.

DING, P. (2024). *A first course in causal inference*. CRC Press.

D’AMOUR, A., DING, P., FELLER, A., LEI, L. and SEKHON, J. (2021). Overlap in observational studies with high-dimensional covariates. *Journal of Econometrics* **221** 644–654.

FENG, P., ZHOU, X.-H., ZOU, Q.-M., FAN, M.-Y. and LI, X.-S. (2012). Generalized propensity score for estimating the average treatment effect of multiple treatments. *Statistics in medicine* **31** 681–697.

FRÖLICH, M. (2004). Programme evaluation with multiple treatments. *Journal of Economic Surveys* **18** 181–224.

GUTMAN, R. and RUBIN, D. B. (2015). Estimation of causal effects of binary treatments in unconfounded studies. *Statistics in medicine* **34** 3381–3398.

HERNAN, M. A. and ROBINS, J. M. (2024). *Causal Inference: What If*. Taylor & Francis, Boca Raton.

HU, L., GU, C., LOPEZ, M., JI, J. and WISNIVESKY, J. (2020). Estimation of causal effects of multiple treatments in observational studies with a binary outcome. *Statistical methods in medical research* **29** 3218–3234.

HU, L., ZOU, J., GU, C., JI, J., LOPEZ, M. and KALE, M. (2022). A flexible sensitivity analysis approach for unmeasured confounding with multiple treatments and a binary outcome with application to SEER-Medicare lung cancer data. *The annals of applied statistics* **16** 1014.

HUBER, M., LECHNER, M. and WUNSCH, C. (2013). The performance of estimators based on the propensity score. *Journal of Econometrics* **175** 1–21.

IMAI, K. and VAN DYK, D. A. (2004). Causal inference with general treatment regimes: Generalizing the propensity score. *Journal of the American Statistical Association* **99** 854–866.

IMBENS, G. W. (2000). The role of the propensity score in estimating dose-response functions. *Biometrika* **87** 706–710.

JIANG, T., GRADUS, J. L. and ROSELLINI, A. J. (2020). Supervised machine learning: a brief primer. *Behavior therapy* **51** 675–687.

JOHNSTONE, I. M. and TITTERINGTON, D. M. (2009). Statistical challenges of high-dimensional data.

KALLUS, N. and ZHOU, A. (2018). Policy evaluation and optimization with continuous treatments. In *International conference on artificial intelligence and statistics* 1243–1251. PMLR.

KERNBACH, J. M. and STAARTJES, V. E. (2022). Foundations of machine learning-based clinical prediction modeling: Part II—Generalization and overfitting. *Machine Learning in Clinical Neuroscience: Foundations and Applications* 15–21.

LI, F. and LI, F. (2019). Propensity score weighting for causal inference with multiple treatments. *The Annals of Applied Statistics* **13** 2389 – 2415. <https://doi.org/10.1214/19-AOAS1282>

LINDEN, A., UYSAL, S. D., RYAN, A. and ADAMS, J. L. (2016). Estimating causal effects for multivalued treatments: a comparison of approaches. *Statistics in Medicine* **35** 534–552.

LOPEZ, M. J. and GUTMAN, R. (2017). Estimation of causal effects with multiple treatments: a review and new ideas. *Statistical Science* 432–454.

MCCAFFREY, D. F., GRIFFIN, B. A., ALMIRALL, D., SLAUGHTER, M. E., RAMCHAND, R. and BURGETTE, L. F. (2013). A tutorial on propensity score estimation for multiple treatments using generalized boosted models. *Statistics in medicine* **32** 3388–3414.

MEHRABI, N., MORSTATTER, F., SAXENA, N., LERMAN, K. and GALSTYAN, A. (2021). A survey on bias and fairness in machine learning. *ACM computing surveys (CSUR)* **54** 1–35.

NEYSHABUR, B., TOMIOKA, R. and SREBRO, N. (2014). In search of the real inductive bias: On the role of implicit regularization in deep learning. *arXiv preprint arXiv:1412.6614*.

QIAN, Z., CURTH, A. and VAN DER SCHAAR, M. (2021). Estimating multi-cause treatment effects via single-cause perturbation. *Advances in Neural Information Processing Systems* **34** 23754–23767.

ROBINS, J. M., ROTNITZKY, A. and ZHAO, L. P. (1995). Analysis of semiparametric regression models for repeated outcomes in the presence of missing data. *Journal of the american statistical association* **90** 106–121.

ROBINSON, P. M. (1988). Root-N-consistent semiparametric regression. *Econometrica: Journal of the Econometric Society* 931–954.

ROSE, S. and NORMAND, S.-L. (2019). Double robust estimation for multiple unordered treatments and clustered observations: evaluating drug-eluting coronary artery stents. *Biometrics* **75** 289–296.

ROSENBAUM, P. R. and RUBIN, D. B. (1983). The central role of the propensity score in observational studies for causal effects. *Biometrika* **70** 41–55.

SIDDIQUE, A. A., SCHNITZER, M. E., BAHAMYIROU, A., WANG, G., HOLTZ, T. H., MIGLIORI, G. B., SOTGIU, G., GANDHI, N. R., VARGAS, M. H., MENZIES, D. et al. (2019). Causal inference with multiple concurrent medications: A comparison of methods and an application in multidrug-resistant tuberculosis. *Statistical methods in medical research* **28** 3534–3549.

TANIMOTO, A., SAKAI, T., TAKENOUCHI, T. and KASHIMA, H. (2021). Regret minimization for causal inference on large treatment space. In *International Conference on Artificial Intelligence and Statistics* 946–954. PMLR.

WAN, F. and MITRA, N. (2018). An evaluation of bias in propensity score-adjusted non-linear regression models. *Statistical methods in medical research* **27** 846–862.

WANG, Y. and BLEI, D. M. (2019). The blessings of multiple causes. *Journal of the American Statistical Association* **114** 1574–1596.

WANG, Y. and BLEI, D. (2021). A proxy variable view of shared confounding. In *International Conference on Machine Learning* 10697–10707. PMLR.

WANG, Y., LI, H., ZHU, M., WU, A., XIONG, R., WU, F. and KUANG, K. (2024). Causal Inference with Complex Treatments: A Survey. *arXiv preprint arXiv:2407.14022*.

WUDIL, U. J., ALIYU, M. H., PRIGMORE, H. L., INGLES, D. J., AHONKHAI, A. A., MUSA, B. M., MUHAMMAD, H., SANI, M. U., NALADO, A. M., ABDU, A. et al. (2021). Apolipoprotein-1 risk variants and associated kidney phenotypes in an adult HIV cohort in Nigeria. *Kidney international* **100** 146–154.

YANG, S., IMBENS, G. W., CUI, Z., FARIES, D. E. and KADZIOLA, Z. (2016). Propensity score matching and subclassification in observational studies with multi-level treatments. *Biometrics* **72** 1055–1065.

ZHOU, T., TONG, G., LI, F., THOMAS, L. E. and LI, F. (2022). PSweight: An R Package for Propensity Score Weighting Analysis. *The R Journal* **14** 282–300. <https://rjournal.github.io/>.

ZHU, Y., COFFMAN, D. L. and GHOSH, D. (2015). A boosting algorithm for estimating generalized propensity scores with continuous treatments. *Journal of causal inference* **3** 25–40.

ZHU, G., WEN, Y., CAO, K., HE, S. and WANG, T. (2024). A review of common statistical methods for dealing with multiple pollutant mixtures and multiple exposures. *Frontiers in Public Health* **12** 1377685.

ZOU, H., CUI, P., LI, B., SHEN, Z., MA, J., YANG, H. and HE, Y. (2020). Counterfactual prediction for bundle treatment. *Advances in Neural Information Processing Systems* **33** 19705–19715.